PCCP

Accepted Manuscript

ROYAL SOCIETY OF CHEMISTRY

www.rsc.org/pccp

N-Confused Porphyrin Tautomers: Lessons from Density Functional Theory†

Gabriel Marchand[*,a], **Hélène Roy**[a], **David Mendive-Tapia**[a], **and Denis Jacquemin**[*,a,b]

Received Xth XXXXXXXXXX 20XX, Accepted Xth XXXXXXXXX 20XX
First published on the web Xth XXXXXXXXXX 200X
DOI: 10.1039/b000000x

Using first-principle calculations, we characterize the properties of N-confused porphyrins (NCP), with a focus on the differences between the 2H and 3H tautomers. NCP-3H is found to be almost as strongly aromatic as porphyrin, and about twice more aromatic, in other words significantly more stable, than NCP-2H, due to the less efficient π-conjugation in the latter form. The deprotonation of the NH-group at the external side of the inverted ring of NCP-2H, which adds a lone pair to the π-system, restores a strong aromaticity, while methylation has no significant effect. Investigating the impact of solvation with a continuum model, we find quite stable solvation energies with a relative dielectric constant, ε_r, in the 5–40 range, for both tautomers. NCP-3H presents a slightly lower energy than its NCP-2H counterpart in all solvents. However, the energy differences between the two species are of the order of the error margin of the method, hence too small to discuss the experimentally observed stabilization of NCP-3H in dichloromethane (DCM, a poorly polar solvent) and NCP-2H in N-N-dimethylformamide (DMF, a highly polar solvent) or to extract the population ratios between the two forms in the different solvents. Therefore, the vibronic absorption spectra are also investigated in an effort to rationalize the complex absorption profiles of these NCP derivatives. We find very distinct spectra for the 2H and 3H forms in DMF and DCM, respectively, each fairly reproducing the experiment. We also find that, in the same solvent, the two species exhibit very different signatures, which allows us to conclude that the 2H and 3H tautomers are largely dominant in DMF and DCM, respectively. Interestingly, the vibrational motions that strongly participate in the overall band shapes, that explains the shoulder of the Soret band and the multiple maxima of the Q-bands, differ in the two tautomers.

1 Introduction

In 1994, the groups of Furuta and Latos-Grażyński independently reported a new porphyrin isomer, the N-confused porphyrin (NCP, see Scheme 1).[1,2] Compared to the canonical porphyrin, the structure of NCP contains an inverted pyrrole ring, the positions of a pyrrole nitrogen and a β-methine pyrrolic group being interchanged. As a direct consequence of this interconversion, NCP presents two stable but non-equivalent tautomeric forms, namely, NCP-3H and NCP-2H (see Scheme 1), while in porphyrin the two most stable tautomers are identical, due to the symmetry of the molecule. NCP-3H is the NCP tautomer containing three hydrogen atoms pointing toward the center of the macrocycle, one of which being part of the central methine group, whereas the two others are bonded to the nitrogens closest to the methine subunit. On the other hand, NCP-2H presents two central hydrogen atoms, the third hydrogen atom being bonded to the nitrogen atom at the external side of the inverted ring.

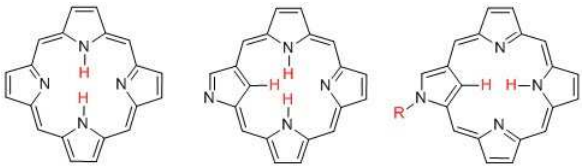

Scheme 1 Left: porphyrin; center: NCP-3H; right: NCP-2H (R=H), Me-NCP-2H (R=Me), and NCP-2H-dep (deprotonated, R=$^-$).

Since its discovery, the tautomeric equilibrium in NCP has attracted a widespread attention from both experimental and theoretical points of view.[3–13]. In 2001, Furuta and coworkers[3] were able to separate the two dominant NCP-3H and NCP-2H species using solvents of different polarities as they could observe distinct absorption spectra. Indeed, NCP-3H could be isolated in dichloromethane (DCM), a poorly polar solvent, while NCP-2H was favored in N-N-dimethylformamide (DMF), a highly polar solvent. A dramatic color change could also be observed in the NCP solu-

† Electronic Supplementary Information (ESI) available: (i) Bond angles; (ii) Delta density plots; (iii) additional computed vibronic absorption spectra; (iv) optimized geometries; (v) vibrational modes' movies. See DOI: 10.1039/b000000x/

[a] *CEISAM, UMR CNRS 6230, BP 92208, Université de Nantes, 2, Rue de la Houssinière, 44322 Nantes, Cedex 3, France. E-mails: gabriel.marchand@univ-nantes.fr; Denis.Jacquemin@univ-nantes.fr*
[b] *Institut Universitaire de France, 103 bd St Michel, 75005 Paris Cedex 5, France.*

tions, red in DCM, green in DMF.

NCP-3H and NCP-2H not only differ in their absorption spectra but also in their structural and magnetic properties. Indeed, X-ray measurements on single crystals revealed that, in contrast to the completely planar geometry of porphyrin, the inverted pyrrole ring is tilted by 4.7° and 26.9° out of the macrocyclic plane in NCP-2H and NCP-3H, respectively,[3] reflecting the smaller electrostatic repulsion between the central hydrogens in NCP-2H. ^{1}H NMR measurements of the inner CH and NH protons performed in $CDCl_3$ revealed chemical shifts in the upfield region at -4.99 and -2.41 ppm, respectively (for NCP-3H). On the other hand, the signals in DMF-d_7 resonated at 0.76, 2.27, and 13.54 ppm (for NCP-2H). The peak in the upfield region at 0.76 ppm was attributed, from the correlation peak with ^{13}C signal, to the inner CH, and the latter two peaks were assigned to the inner and outer NH.[3] One likely explanation for such modest upfield shifts of the central CH and NH in NCP-2H is the weak diamagnetic ring current owing to the ineffective conjugation of the π-system.

Beyond the examination of the two predominant NCP-3H and NCP-2H compounds, additional NCP tautomeric forms have catched special interest. In particular, the external NH-group on the inverted pyrrole ring in NCP-2H can be readily deprotonated using a strong liquid base leading to NCP-2H-dep,[4] see Scheme 1. This creates an additional lone pair that can participate in the π-conjugated network. The 2H tautomeric structure can also be forced by alkylation on the external nitrogen with a methyl group (Me-NCP-2H in Scheme 1).[5,6]

The relative stabilities of NCP-3H and NCP-2H, as well as of other structural isomers, have been previously discussed using density functional theory (DFT) calculations of the electronic ground state energies in gas phase.[7–10]. All these previous works found an energetic preference for NCP-3H, the difference with NCP-2H being of ca. 5 kcal.mol^{-1}, which is within the error of the method, hinting that the two tautomers can be hardly distinguished on the basis of their ground state energies. One way to rationalize the relative stability of the two tautomers is to quantify their aromatic pattern *via* NICS (nuclear independent chemical shift) simulations.[14] However, to the best of our knowledge, NICS has been reported for the 3H tautomer only.[11] Furthermore, although the experimental absorption data are abundant,[3,4,9,10,12] no vibrationally resolved absorption spectra has been yet simulated in order to characterize the more important vibrational modes explaining the specific band topologies of NCP.

Thus, a more complete picture of the chemistry of the two predominant NCP tautomers using first-principle tools needs to be addressed, and this is the aim of this contribution. First, the relative stabilities of NCP-3H and NCP-2H, as well as NCP-2H-dep and Me-NCP-2H, the deprotonated and methylated forms of NCP-2H, are discussed by investigating both their structures and their aromaticity patterns in all the cycles. This allows us to revisit the effect of the hydrogen repulsion at the center on the geometries, i.e., on the bond lengths, angles, and dihedrals. Furthermore, we investigate the correlation between the bond patterns in a given cycle and the (anti)aromaticity of this cycle, as measured by NICS. Second, the relative stabilities of NCP-3H and NCP-2H are further examined by means of their electronic ground states energies in a large panel of solvents presenting various polarities. Finally, the vibrationally resolved absorption spectra of NCP-3H and NCP-2H are presented for the first time.

2 Computational Methods

All our calculations have been performed at the DFT and TD-DFT levels using the Gaussian 09 software,[15] applying default procedures, integration grids and algorithms, apart from tightened energy (10^{-10} a.u.) and internal forces (10^{-5} a.u.) convergence thresholds. Except where noted, calculations were carried out with the M06-2X meta-hybrid exchange-correlation functional,[16] which is a recommended choice for many properties, including excited-state simulations.[16–18] The geometries of the singlet electronic ground state and the first four singlet electronic excited states of the NCP molecules have been optimized at the M06-2X/6-31G(d) level. Bulk solvent effects were estimated using the polarizable continuum model (PCM). No imaginary frequencies were obtained after vibrational analysis on the optimized structures, and additional single-points using the 6-31++G(d,p) atomic basis set were carried out to correct the energies. To account for the perturbation of the PCM polarization when the solute reaches an excited state, we used the equilibrium state-specific solvation scheme[19] and the corrected linear response (cLR) formalism in its non-equilibrium limit[20] for adiabatic and vertical transition energies, respectively.

The aromaticity was quantified *via* (singlet electronic ground state) calculations of the NICS(0)[14] at the centers of all the rings. Note that most experimentally available N-confused porphyrins contain four phenyl rings as external substituents. These phenyl rings are almost perfectly perpendicular with the NCP core, and do not play an important role (see discussion in Ref. 10). Here, we have chosen to use only hydrogen-capped NCP to allow the simulation of the vibronic spectra. To this end, we used the time-independent (frequency domain) method implemented in the FCclasses code[21,22], considering the equilibrium geometries and normal modes of both the ground state and the excited state. This method relies upon the harmonic potential approximation, which is suitable for reasonably low degree of vibrational excitation. Originally limited to cases where the transition dipole moment between the two given states can be considered independent of the nuclear coordinates (Condon approximation), it has been extended to

the more general Herzberg-Teller (HT) model, thus allowing the investigation of weak and vibronically allowed transitions with small Franck-Condon factors.

The vibronic spectra of NCP-3H and NCP-2H in DCM and DMF were simulated taking into account the first four excited states, applying the Condon approximation for strongly allowed transitions (so-called Franck-Condon (FC) spectra), and adding the HT effects for weakly allowed transitions. Strong and weak transitions were arbitrarily splitted according to the oscillator strength value (above or below 0.1). The temperature effects (T= 298 K) were integrated, and the number of integrals was adjusted so to recover a fraction of the FC or the full (FC + HT) spectrum exceeding 90%. In order to investigate the effect of the polarity of the solvent on the stability of NCP-2H and NCP-3H, solvation energies were estimated from (singlet ground state) single-point calculations using the solvation model density (SMD)[23] based on the optimized geometries in gas phase.

3 Results and discussion

3.1 Structure and aromaticity

Fig. 1 evidences the structural deformation of NCP-3H resulting from the steric congestion imposed by the additional hydrogen atom in the core. More specifically, the N-confused cycle is tilted out of the macrocycle plane by ca. 20°, which contrasts to the completely planar geometry of porphyrin. Despite this conformational relaxation, a significant hydrogen-hydrogen repulsion persists in NCP-3H as the average distance between the three central hydrogens (2.36 Å for the NH−−HN distance and 1.86 Å for the two CH−−HN distances) is significantly smaller than 2.17 Å, the NH−−HN distance in porphyrin. This is illustrated in Fig. 2. The C_α-N-H angles of NCP-3H are also affected (see Fig. S1 in the Electronic Supplementary Information (ESI)), the two external C_α-N-H angles (120.8°) being smaller than the two internal C_α-N-H angles (127.4°). For comparison, the four (equal) C_α-N-H angles of porphyrin are of 124.7°. Beyond these differences, the bond lengths in the 16-membered ring of porphyrin and NCP-3H are very similar (see Fig. 2). The C-C bonds are typically 1.39 Å long in both molecules, which is 0.15 Å smaller and 0.04 Å larger than normal single and double carbon bonds, respectively, and equivalent to benzene, another highly aromatic compound.

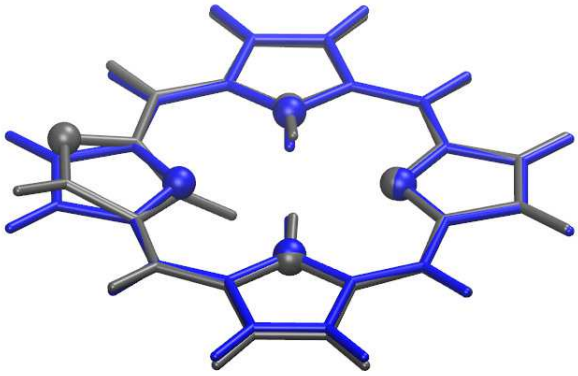

Fig. 1 3D structures of porphyrin (blue) and NCP-3H (gray) optimized in their electronic ground states. Nitrogen atoms are represented as spheres.

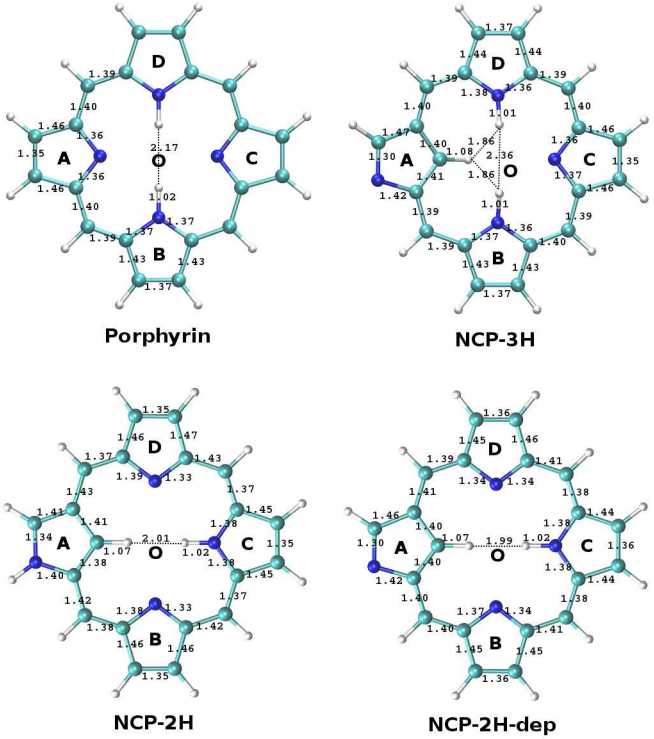

Fig. 2 Bond lengths (Å) in porphyrin and the selected N-confused analogues in their optimized electronic ground states. O, A, B, C, and D: naming convention for the cycles.

Although there is no extra hydrogen at the center of NCP-2H, its structure is intermediate between porphyrin and NCP-3H as it presents a slight out-of-plane deformation of ca. 5°. We underline that the simulated torsion angles of the two NCP tautomers correlate well with the 26.9° and 4.7° values reported from X-ray diffraction of tetraphenyl NCP-3H and NCP-2H, respectively,[3] confirming the not very important role played by the phenyl groups. The two central hydrogens in NCP-2H are separated by 2.01 Å (see Fig. 2), that is 0.16 Å smaller than in porphyrin and 0.15 Å larger than the

CH−−HN distances in NCP-3H. This reduced distance *versus* porphyrin is related to: i) the larger C-H bond of NCP-2H (1.07 Å) compared to the N-H bonds in both molecules (1.02 Å); ii) the larger C_α-C and C_α-N bonds in NCP-2H (from 1.38 to 1.41 Å) compared to the C_α-N bonds in porphyrin (1.37 Å); and iii) the more acute C_α-C-C_α angle in NCP-2H (108.6°) compared to the C_α-N-C_α angles in porphyrin (110.6°) and NCP-2H (110.8°), see Fig. S1 in the ESI. Relative to NCP-3H, the stability of NCP-2H suffers, in counterpart of its reduced steric stress, from a less effective π-delocalization. This can be seen from the unequal bonds in the macrocycle, with minimum and maximum lengths of 1.33 and 1.43 Å (see Fig. 2). No significant difference could be detected when superimposing the structures of NCP-2H and its deprotonated analogue, NCP-2H-dep, both compounds showing their confused cycle distorted out of the macrocyclic plane by $\sim 5°$. However, the deprotonation has the effect of uniformizing the bond distances (compare NCP-2H and NCP-2H-dep in Fig. 2), the distribution becoming similar to that of NCP-3H. As for the methylated form Me-NCP-2H (not shown), we found no difference with respect to NCP-2H.

One way to examine the relative stability of porphyrin and its N-confused isomers is to quantify their (anti)aromaticity by calculations of the NICS at the centers of the cycles, see the computational methods section. Of course, equal and unequal bond lengths are likely to favor aromaticity and antiaromaticity, respectively. The NICS values may thus correlate with the bond distributions, that we have characterized using the standard deviation σ (in Å):

$$\sigma_i = \left[\sum_j (r_{i,j} - \langle r_i \rangle)^2\right]^{1/2},$$

where $r_{i,j}$ is the length of bond j in cycle i and $\langle r_i \rangle$ is the average bond length in that cycle. We underline that the NICS and σ are not the unique criteria (we redirect the interest reader to the works of von Schleyer[14,24]) to predict the aromatic behavior of a given compound. Fig. 3 shows the correlation between NICS and σ for all the rings. The numerical values are available in Table 1. In Fig. 3, one can see a clear, roughly linear, dependency between these two quantities. The smaller is the geometrical deviation, the smaller is the NICS, and the stronger is the aromaticity. This is true for both the macrocycle and the peripheral rings (excluding A and O of NCP-2H and Me-NCP-2H, the non-conjugated rings, see the labels of the rings in Fig. 2). The macrocycle and the five-member rings follow a different slope, suggesting that other parameters than σ like the size or the nature of the ring can also affect the NICS. At the opposite, adding or changing the solvent does not affect significantly the aromaticity since comparable values are obtained when computing the NICS in gas phase, DCM and DMF (see Table S1 in the ESI). In addition, for

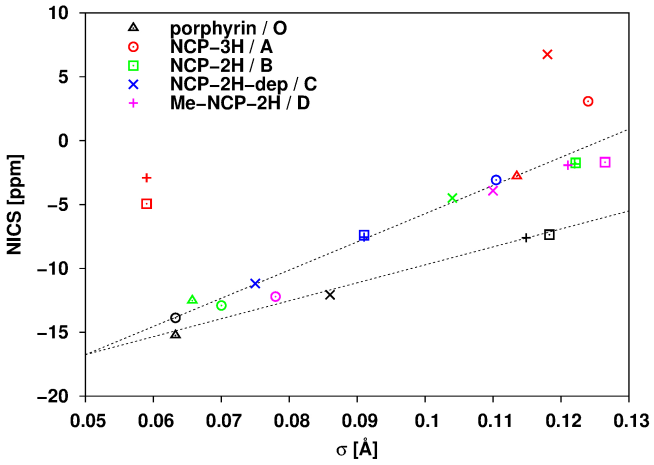

Fig. 3 NICS (in ppm) *versus* the standard deviation σ (in Å) of the bond length distribution, for all the cycles in porphyrin and the selected NCP molecules (see the denomination of the compounds and the rings in Scheme 1 and Fig. 2). Symbols refer to the molecules and colors refer to the rings.

Table 1 NICS (ppm) and σ values (Å) for all the rings (see the labels of the rings in Fig. 2).

	NICS					$\sigma * 10$				
	O	A	B	C	D	O	A	B	C	D
porphyrin	-15.2	-2.8	-12.5	-2.8	-12.5	0.63	1.13	0.66	1.13	0.66
NCP-3H	-13.9	3.1	-12.9	-3.1	-12.2	0.63	1.24	0.70	1.10	0.78
NCP-2H	-7.4	-4.9	-1.7	-7.4	-1.7	1.18	0.59	1.22	0.91	1.26
NCP-2H-dep	-12.1	6.8	-4.5	-11.2	-3.9	0.86	1.18	1.04	0.75	1.10
Me-NCP-2H	-7.6	-2.9	-1.8	-7.5	-1.9	1.15	0.59	1.22	0.91	1.21

NCP-3H, the presented NICS values are in close agreement with those obtained at the HF/6-31+G(d)//B3LYP/6-31G(d) level in gas phase.[11]

As it can be seen in Table 1, all the cycles of porphyrin, NCP-2H, and Me-NCP-2H are aromatic (NICS < 0) while NCP-3H and NCP-2H-dep exhibit respectively a non-aromatic (NICS around 0) and antiaromatic (NICS > 0) character for their inverted cycle A, most probably because of the relatively high electronic density on the nitrogen atom in that particular ring. Porphyrin and NCP-3H are both conjugated and have similar deviations in their bond length distributions (excluding ring A), they also develop similar aromatic patterns. These two compounds are highly aromatic since their NICS values at the center are strongly negative, -15.3 ppm in porphyrin and -13.9 ppm in NCP-3H. This is about twice larger than in both NCP-2H and Me-NCP-2H (-7.5 ppm, a value close to the one found in benzene).[14] This shows evidence that NCP-3H is significantly more stable than its NCP-2H analogue, because of the more efficient π-delocalization and despite the stronger hydrogenic repulsion at the center in the 3H form. Likewise, the aromaticity of the five-member

rings in porphyrin and NCP-3H is roughly twice more pronounced than in NCP-2H and Me-NCP-2H (comparing rings of same topology and, again, excluding A of NCP-3H). Upon deprotonation of its confused pyrrole, the created lone pair "repairs" the π-delocalization as NCP-2H-dep is almost as aromatic as porphyrin and NCP-3H. The gain of aromaticity from NCP-2H to NCP-2H-dep is also substantial on the peripheral B, C, and D rings. The methylation, on the other hand, destabilizes only slightly its local environment (see the NICS of rings A of NCP-2H and Me-NCP-2H in Table 1).

3.2 Energy of NCP-2H and NCP-3H *versus* the solvent polarity

As stated in the introduction, the two dominant tautomers of N-confused porphyrin, NCP-2H and NCP-3H, can be separated experimentally using solvents of different polarities, the 2H and 3H forms being stabilized in DMF and DCM, respectively.[3] We have shown above from NICS simulations that NCP-3H is about twice more aromatic, hence significantly more stable, than NCP-2H, independently of the presence (or not) of the DCM and DMF solvents. In this part, we further examine whether the relative stabilities of these two tautomers can be quantified from their electronic ground state free energies in solvents of different polarities, using:

$$G = G_{\text{gas}} + G_{\text{solv}},$$

where G_{gas} is the Gibbs free energy in gas phase and G_{solv} is the solvation free energy estimated through a single-point energy calculation with the SMD model (see previous section). In very good agreement with the values reported in previous theoretical works[7–10], we find that, in gas phase, the free energy G_{gas} of NCP-3H is 4.98 kcal.mol^{-1} lower than the one of NCP-2H. Such a very small energy is difficult to interpret since it is close to the DFT uncertainty threshold.

The G-values were calculated using a wide panel of solvents presenting relative dielectric constants ε_r ranging from 2 to 110, and considering both protic and aprotic solvents (see Fig. 4). Very similar energy-curves are found for the two tautomers, both displaying higher energies in strongly apolar solvents (ca. $\varepsilon_r < 5$) and polar solvents (ca. $\varepsilon_r > 40$), a region of greater stabilization being obtained in the intermediate range (ε_r going from 5 to 40) considering arbitrarily, $G <$ 4 kcal.mol^{-1}. In all the selected solvents, the energy of NCP-3H is below the one of NCP-2H, both tautomers having their lowest energies in DCM. In other words, we do not observe an inversion of the energy-curves of the two species when varying the polarity of the solvent. In fact, adding the solvent reduces the energy difference between the two tautomers to ca. 0.5–4.0 kcal.mol^{-1}, depending on the solvent. Such energies are trifling, showing that it is very difficult to discuss the stabilities of NCP-3H and NCP-2H in this manner.

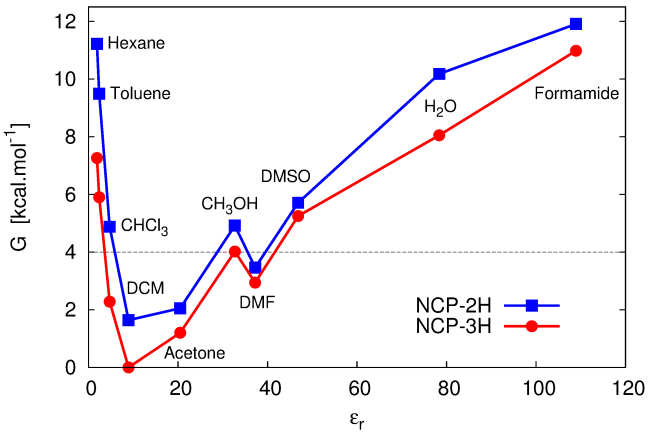

Fig. 4 Relative free energies G of NCP-2H and NCP-3H as a function of the relative dielectric constant of the solvent, ε_r.

3.3 Absorption spectra

Table 2 presents the vertical absorption data obtained for the different macrocycles considered here. All compounds show two weakly dipole-allowed transitions at small energy (giving rise to the Q-bands) and two strongly dipole-allowed transitions at higher energy (corresponding to the Soret bands). In this sense, N-confusion only tunes the nature of the excited states of the reference porphyrin but does not change the major features of the optical spectrum. It is obvious from the data in Table 2 that all NCP isomers present smaller transition energies for the Soret band, the shift being ca. -0.25 eV. The total computed intensity for those transitions is also smaller in the NCP compounds than in the canonical porphyrin. The S_1 appears at a particularly small energy in NCP-3H (ca. 0.1/0.2 eV lower than in NCP-2H/porphyrin) and is weakly intense. In NCP-2H, the separation between the two Q excited states is significantly larger than in porphyrin and NCP-3H, but this effect is completely annihilated in the corresponding deprotonated form. We also note that, as for the other properties investigated here, Me-NCP-2H and NCP-2H present very similar excited-state energies. In order to obtain further insights regarding the nature of the excited states of NCP-2H and NCP-3H, we provide electron density difference plots correspond-

Table 2 Vertical transition energies (E in eV) and oscillator strengths (f) for the first four singlet excited states.

	S_1		S_2		S_3		S_4	
	E (eV)	f	E (eV)	f	E (eV)	f	E (eV)	f
Porphyrin	2.310	0.001	2.547	0.004	3.649	1.303	3.734	1.460
NCP-3H	2.107	0.012	2.423	0.002	3.323	0.962	3.465	1.230
NCP-2H	2.248	0.076	2.663	0.023	3.507	1.246	3.529	0.640
NCP-2H-dep	2.223	0.084	2.377	0.002	3.283	0.937	3.434	1.237
Me-NCP-2H	2.212	0.066	2.619	0.031	3.441	1.232	3.449	0.633

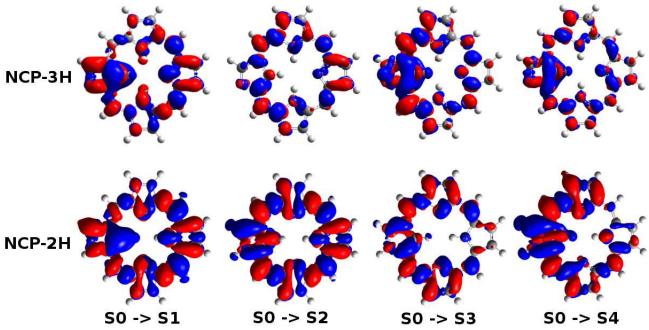

Fig. 5 Electronic density difference between the first four excited states and the ground state. Red (blue) regions indicate increase (decrease) of electron density upon absorption of light.

ing to the four lowest-lying excited states in Fig. 5 (see Fig. S2 in the ESI for NCP-2H-dep and Me-NCP-2H). One can see from these plots that the electron density tends to reorganize across the whole molecule but with a stronger variation in the inverted ring region (especially for the $S_0 \rightarrow S_3$ and $S_0 \rightarrow S_4$ Soret transitions that are strongly asymmetric), for all the NCP forms presented here. As typical of valence π-excited states, the reorganization is constituted of an alternation of gain and depletion of density, following the nature of the bonds (see Fig. 2). The $S_0 \rightarrow S_1$ reorganization is similar in NCP-3H and NCP-2H, the internal methine group obviously loosing significant density (donor). It is also remarkable that the density fluctuations induced by the $S_0 \rightarrow S_1$ and $S_0 \rightarrow S_2$ transitions are more important in NCP-2H than in NCP-3H, which indicates that the more strongly dipole-allowed transitions correspond to Q-bands implying a stronger reorganization. Eventually, as it can be seen by comparing Figs. 5 and S2, the electronic reorganization of NCP-2H-dep and Me-NCP-2H is similar to their NCP-3H and NCP-2H counterparts.

The vibronic absorption spectra of NCP-3H in DCM and NCP-2H in DMF were simulated and the results are shown in Fig. 6. The position and height of the Soret band have been adjusted to the experimental curve in order to allow a straightforward comparison. In agreement with the experimental data, the two tautomers exhibit distinct signatures. The correspondence between theory and experiment is rather satisfying for both molecules, though TD-DFT underestimates the absorption wavelength of the first Q-band (originating from the first excited state, see the decomposed spectrum in Fig. S3 in the ESI) in NCP-3H. The Soret band and its shoulder at small wavelengths are nicely reproduced. The shape and relative intensity of the Q-bands, compared to the intense Soret band, also correlate well with the experiment. Moreover, the calculation of the vibronic absorption spectrum of NCP-3H in the DMF polar solvent (see Fig. S4 in the ESI) leads to a profile very divergent from that of NCP-2H in the same medium. We

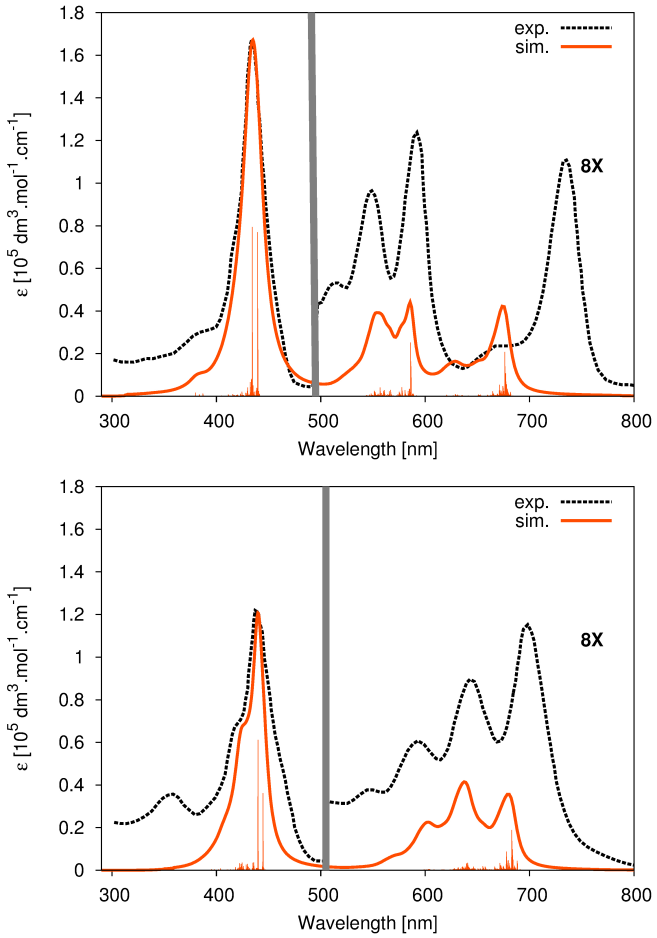

Fig. 6 Vibrationally resolved absorption spectra together with the individual stick contributions of the vibrations for NCP-3H in DCM (top) and NCP-2H in DMF (bottom), and comparison with experimental data. The theoretical curve is the sum of the contributions of the first four excited states. It has been shifted such that the position and height of the Soret band coincide with the experimental one. The shift in the *x*-axis is 60/80 nm for NCP-3H/NCP-2H. The experimental spectra is adapted with permission from Ziegler *et al.*, *J. Phys. Chem. A* **2013**, *117*, 11499–11508. Copyright 2013 American Chemical Society.

can thus conclude from these simulated spectra that the experimental NCP solutions in DCM and DMF must be mostly populated by the NCP-3H and the NCP-2H species, respectively. The immersion of NCP-3H in DMF also has the effect, compared to the less polar DCM, of splitting the sharp Soret band in a wider and less intense "doublet" band, and more remarkably, of strongly decreasing the intensity of the first Q-band.

In both molecules, we find, as expected, that the strongly allowed Soret peak originates from the E_{0-0} transitions to the almost degenerated S_3 and S_4 states (see the absorption

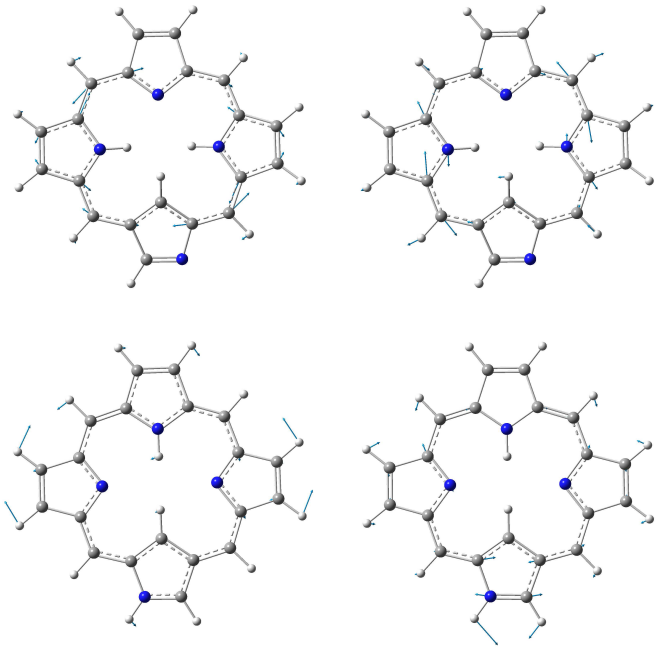

Fig. 7 Vibrational normal modes that strongly contribute to the shoulder of the Soret band. Top: NCP-3H (left: 2087 cm^{-1}; right: 2271 cm^{-1}); bottom: NCP-2H (left: 1312 cm^{-1}; right: 1598 cm^{-1}).

bands for S_3 and S_4 in Fig. S3). As required by the Franck-Condon principle, S_0, S_3, and S_4 exhibit very similar equilibrium geometries (see Fig. S5 for NCP-3H as an example in the ESI). At the opposite, the shoulder of the Soret band at ca. 380/425 nm for NCP-3H/NCP-2H arises from a combination of various vibrational motions. In particular, two vibrational modes at 2088 and 2271 cm^{-1} strongly participate in the shoulder of NCP-3H, both consisting of a collection of stretching and bending modes involving carbon and nitrogen atoms along the macrocycle (see Fig. 7 and the movies in the ESI). Surprisingly, the Soret shoulders in NCP-2H and NCP-3H do not share the same origin as the nuclear displacements mostly responsible for the shoulder of NCP-2H are largely dominated by balancing motions of the peripheral hydrogens in the macrocyclic plane and with corresponding frequencies of 1312 and 1598 cm^{-1}.

The Herzberg-Teller effects play a crucial role in the Q-band at ca. 555/635 nm in NCP-3H/NCP-2H. These vibronically allowed shapes are related to a large panel of vibrations in both molecules, nonetheless, the most intense contributions can be identified. The band at 555 nm in NCP-3H can be associated to large oscillations in the macrocyclic plane at 1125 cm^{-1} involving hydrogens at the periphery, see Fig. 8. For the band at 635 nm in NCP-2H, two peaks almost equal in intensity are found at 1248 and 1282 cm^{-1}, both dominated by hydrogenic displacements in phase (opposite phase) at the exterior (center) of the macrocycle, see Fig. 8. We also note that the optimized geometries of S_1 and S_2 differ slightly from the one of S_0, and that the photoinduced deformations correlate well, as it could be expected, with the nuclear displacements along these important vibrational modes in the excited state (see Fig. S5 and the movies in the ESI).

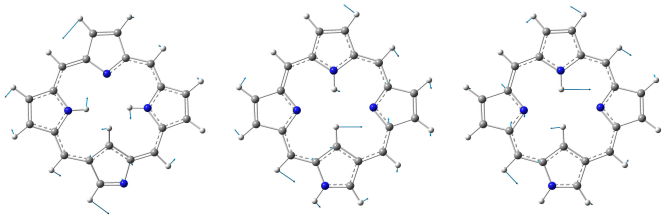

Fig. 8 Vibrational normal modes that strongly contribute to the Q-band at 555 nm in NCP-3H (left) and 635 nm in NCP-2H (center and right).

4 Conclusion and Outlook

In summary, the NH tautomerism of N-confused porphyrin has been revisited using first-principle calculations, with a particular attention on the NCP-3H and NCP-2H tautomers, the two most stable forms. We show that the extra (missing) central hydrogen in NCP-3H (NCP-2H) considerably affects the equilibrium molecular geometries. Despite its greater steric hindrance, NCP-3H is found to be almost as strongly aromatic as the reference porphyrin, hence very stable, and about twice more aromatic than its 2H analogue, due to the less efficient π-system in the latter form. The aromatic strength of NCP-2H can however be increased up to almost the same degree as in NCP-3H *via* the deprotonation of the external NH group that creates a lone pair of electrons able to participate in the π-conjugation. As for the other properties investigated here, the methylation of NCP-2H has almost no effect on its stability. The ground state energies of NCP-3H and NCP-2H in gas phase are found to be different by 5 $kcal.mol^{-1}$ only, which is in agreement with previous DFT computational studies and close to the limit of what can be detected with this method. Investigating the effect of solvation using a continuum model in a large panel of solvents with various polarities, we find quite stable energies with a relative dielectric constant in the 5–40 range for both tautomers, DCM being the most stabilizing medium. NCP-3H presents slightly lower energy than its NCP-2H counterpart in all the solvents investigated here. However, the energy differences between the two molecules are trifling: in the 0.5–4 $kcal.mol^{-1}$ range, showing that it is difficult to discuss the experimentally observed stabilization of NCP-3H in DCM and NCP-2H in DMF in this manner.

The theoretical vibronic absorption spectra of both

molecules have been computed for the first time. The simulations of NCP-3H in DCM and NCP-2H in DMF lead to distinct signatures that fairly well reproduce the experimental UV/Vis data of the NCP compound immersed in these two solvents. Beyond that, the simulation of the spectrum of NCP-3H in DMF yields a very different profile compared to NCP-2H in the same solvent. We can thus conclude that the 3H and 2H tautomers are each to each largely dominant in DCM and DMF. The influence of the nature of the solvent is also seen when comparing the spectral features of the 3H tautomer in the two solvents: the Soret band in DCM being splitted into a wider and weaker "doublet" band upon immersion in DMF, while the intensity of the Q-band at largest wavelengths is strongly reduced. Identifying the vibrational normal modes playing an important role in the non 0-0 transitions, i.e., the Soret shoulder and the high-energy Q-bands, we find that the corresponding nuclear motions are surprisingly not the same for the two tautomers.

Acknowledgment

All authors are indebted to Dr. A. D. Laurent and MSc C. D. Sergentu for many fruitful discussions. G. M. thanks the *Région des Pays de la Loire* for his post-doctoral grant in the framework of the SAPOMAP project. D. M. T. thanks the European Research Council (ERC, Marches - 278845) for his post-doctoral grant. D. J. acknowledges the European Research Council (ERC) and the *Région des Pays de la Loire* for financial support in the framework of a Starting Grant (Marches - 278845) and the SAPOMAP project. This research used resources of the GENCI-CINES/IDRIS (Grant c2014085117), CCIPL (*Centre de Calcul Intensif des Pays de Loire*), and a local Troy cluster.

References

1 H. Furuta, T. Asano and O. T., *J. Am. Chem. Soc.*, 1994, **116**, 767–768.
2 P. J. Chmielewski, L. Latos-Grażyński, K. Rachlewicz and T. Glowiak, 1994, **33**, 779–781.
3 H. Furuta, T. Ishizuka, A. Osuka, H. Dejima, H. Nakagawa and Y. Ishikawa, *J. Am. Chem. Soc.*, 2001, **123**, 6207–6208.
4 C. J. Ziegler, N. R. Erickson, M. R. Dahlby and V. N. Nemykin, *J. Phys. Chem. A*, 2013, **117**, 11499–11508.
5 E. A. Alemán, C. S. Rajesh, C. S. Ziegler and D. A. Modarelli, *J. Phys. Chem. A*, 2006, **110**, 8605–8612.
6 P. Chmielewski and L. Latos-Grażyński, *J. Chem. Soc., Perkin Trans. 2*, 1995, 503–509.
7 L. Szterenberg and L. Latos-Grażyński, *Inorg. Chem.*, 1997, **36**, 6287–6291.
8 A. Ghosh, T. Wondimagegn and H. J. Nilsen, *J. Phys. Chem. B*, 1998, **102**, 10459–10467.
9 J. P. Belair, C. J. Ziegler, C. S. Rajesh and D. A. Modarelli, *J. Phys. Chem. A*, 2002, **106**, 6445–6451.
10 S. Vyas, C. M. Hadad and D. A. Modarelli, *J. Phys. Chem. A*, 2008, **112**, 6533–6549.
11 B. Kiran and M. T. Nguyen, *J. Organomet. Chem.*, 2002, **643-644**, 265–271.
12 S. Sripothongnak, C. J. Ziegler, M. R. Dahlby and V. N. Nemykin, *Inorg. Chem.*, 2011, **50**, 6902–6909.
13 H. Maeda and H. Furuta, *Pure Appl. Chem.*, 2006, **78**, 29–44.
14 Z. Chen, C. S. Wannere, C. Corminboeuf, R. Puchta and P. v. R. Schleyer, *Chem. Rev.*, 2005, **105**, 3842–3888.
15 M. J. Frisch, G. W. Trucks, H. B. Schlegel, G. E. Scuseria, M. A. Robb, J. R. Cheeseman, G. Scalmani, V. Barone, B. Mennucci, G. A. Petersson, H. Nakatsuji, M. Caricato, X. Li, H. P. Hratchian, A. F. Izmaylov, J. Bloino, G. Zheng, J. L. Sonnenberg, M. Hada, M. Ehara, K. Toyota, R. Fukuda, J. Hasegawa, M. Ishida, T. Nakajima, Y. Honda, O. Kitao, H. Nakai, T. Vreven, J. A. Montgomery, Jr., J. E. Peralta, F. Ogliaro, M. Bearpark, J. J. Heyd, E. Brothers, K. N. Kudin, V. N. Staroverov, R. Kobayashi, J. Normand, K. Raghavachari, A. Rendell, J. C. Burant, S. S. Iyengar, J. Tomasi, M. Cossi, N. Rega, J. M. Millam, M. Klene, J. E. Knox, J. B. Cross, V. Bakken, C. Adamo, J. Jaramillo, R. Gomperts, R. E. Stratmann, O. Yazyev, A. J. Austin, R. Cammi, C. Pomelli, J. W. Ochterski, R. L. Martin, K. Morokuma, V. G. Zakrzewski, G. A. Voth, P. Salvador, J. J. Dannenberg, S. Dapprich, A. D. Daniels, Ã. Farkas, J. B. Foresman, J. V. Ortiz, J. Cioslowski and D. J. Fox, *Gaussian 09 Revision A.02*, Gaussian Inc. Wallingford CT 2009.
16 Y. Zhao and D. G. Truhlar, *Theor. Chem. Acc.*, 2008, **120**, 215–241.
17 Y. Zhao and D. G. Truhlar, *Acc. Chem. Res.*, 2008, **41**, 157–167.
18 D. Jacquemin, A. Planchat, C. Adamo and B. Mennucci, *J. Chem. Theory Comput.*, 2012, **8**, 2359–2372.
19 R. Improta, V. Barone, G. Scalmani and M. J. Frisch, *J. Chem. Phys.*, 2006, **125**, 054103.
20 M. Caricato, B. Mennucci, J. Tomasi, F. Ingrosso, R. Cammi, S. Corni and G. Scalmani, *J. Chem. Phys.*, 2006, **124**, 124520.
21 F. Santoro, A. Lami, R. Improta, J. Bloino and V. Barone, *J. Chem. Phys.*, 2008, **128**, 224311.
22 F. Santoro, *"FCclasses, a Fortran 77 code": visit http://village.ipcf.cnr.it*.
23 A. V. Marenich, C. J. Cramer and D. G. Truhlar, *J. Phys. Chem. B*, 2009, **113**, 6378–6396.
24 C. S. Wannere, K. W. Sattelmeyer, I. H. F. Schaefer and P. v. R. Schleyer, *Angew. Chem. Int. Ed.*, 2004, **43**, 4200–4206.

Graphical Abstract

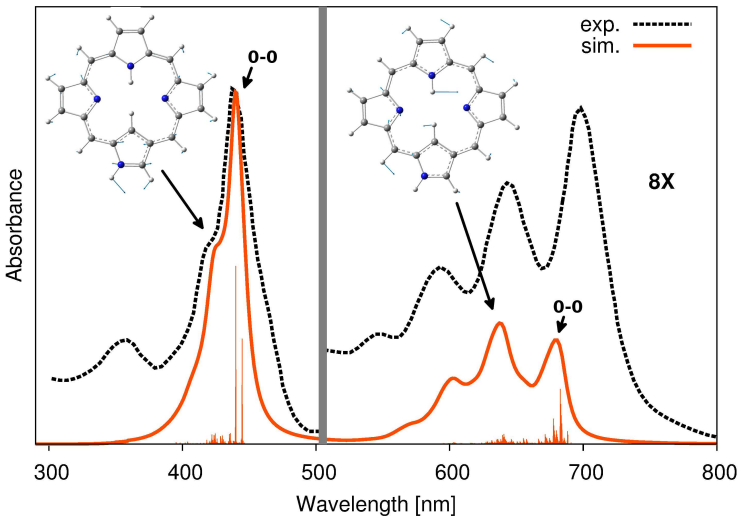

In this paper, the complex UV/Vis absorption signature of the dominant N-confused porphyrin tautomers is rationalized by simulations of the vibrationally resolved spectra.